Fungal Genetics and Biology 165 (2023) 103768

Contents lists available at ScienceDirect

Fungal Genetics and Biology

journal homepage: www.elsevier.com/locate/yfgbi

Septum-associated microtubule organizing centers within conidia support infectious development by the blast fungus *Magnaporthe oryzae*

Audra Mae Rogers, Martin John Egan *

Department of Entomology and Plant Pathology, University of Arkansas, Fayetteville, AR 72701, USA

ARTICLE INFO

Keywords:
Appressoria
Blast
Microtubules
EB1
Mitosis

ABSTRACT

Cytoplasmic microtubule arrays play important and diverse roles within fungal cells, including serving as molecular highways for motor-driven organelle motility. While the dynamic plus ends of cytoplasmic microtubules are free to explore the cytoplasm through their stochastic growth and shrinkage, their minus ends are nucleated at discrete organizing centers, composed of large multi-subunit protein complexes. The location and composition of these microtubule organizing centers varies depending on genus, cell type, and in some instances cell-cycle stage. Despite their obvious importance, our understanding of the nature, diversity, and regulation of microtubule organizing centers in fungi remains incomplete. Here, using three-color fluorescence microscopy based live-cell imaging, we investigate the organization and dynamic behavior of the microtubule cytoskeleton within infection-related cell types of the filamentous fungus, *Magnaporthe oryzae*, a highly destructive pathogen of rice and wheat. We provide data to support the idea that cytoplasmic microtubules are nucleated at septa, rather than at nuclear spindle pole bodies, within the three-celled blast conidium, and provide new insight into remodeling of the microtubule cytoskeleton during nuclear division and inheritance. Lastly, we provide a more complete picture of the architecture and subcellular organization of the prototypical blast appressorium, a specialized pressure-generating cell type used to invade host tissue. Taken together, our study provides new insight into microtubule nucleation, organization, and dynamics in specialized and differentiated fungal cell types.

1. Introduction

The filamentous fungus *Magnporthe oryzae* (synonym *Pyricularia oryzae*) causes a destructive disease of cultivated rice and wheat, called blast, which threatens food security around the world. Blast infections begin when an asexual spore, called a conidium, lands on the leaf surface following its dispersal from nearby infected tissue. *M. oryzae* conidia are pyriform in shape and composed of three discrete cells (referred to here as apical, middle, and terminal) interconnected via two septal pores (Money and Howard, 1996), and each cell of the conidium contains a single nucleus (Veneault-Fourrey et al., 2006). In the presence of free water, and in the absence of external nutrients, within a couple of hours the conidium produces a narrow germ tube which can emerge from any one of the three cells of the conidium, although most often this is from the apical cell. The polarized germ tube extends a short distance across the cuticle, where it perceives various host-derived chemical and physical cues which influence the commitment to terminal differentiation (Anjago et al., 2018). Under conducive conditions, a complex morphogenetic program is initiated, leading to the differentiation of a specialized dome-shaped infection cell called an appressorium, at the apex of the germ tube (Ryder et al., 2022). The *M. oryzae* appressorium is a remarkable cell type in that it can generate enormous turgor pressure, and, owing to its specialized subcellular architecture (Dagdas et al., 2012), use this pressure to force a narrow hyphal protrusion, emerging from its base, through the tough leaf cuticle. As it matures, the appressorium generates increasing hydrostatic pressure through the intracellular accumulation of glycerol, and other osmolytes, mobilized from the conidium, which causes water to enter the infection cell by osmosis (de Jong et al., 1997). Recent data suggests that the production, and detection, of sufficient turgor pressure within the appressorium, monitored by a resident histidine-aspartate sensor kinase (Ryder et al., 2019), triggers the F-actin and microtubule-dependent remodeling of a septin disc within the base of the appressorium into a ring-like structure that is essential for appressorium functionality (Dagdas et al., 2012; Dulal et al., 2021, 2020). The regulated production of reactive oxygen species by one of three NADPH oxidase enzymes encoded by the *M. oryzae* genome, Nox2, is also essential for remodeling of the septin cytoskeleton, likely through the oxidative modification of an F-actin regulatory

* Corresponding author.
E-mail address: me021@uark.edu (M.J. Egan).

https://doi.org/10.1016/j.fgb.2022.103768
Received 19 September 2022; Received in revised form 16 December 2022; Accepted 22 December 2022
Available online 31 December 2022

protein (Egan et al., 2007; Ryder et al., 2013).

Importantly, appressorium development is tightly coupled to cell-cycle progression, and monitored by a canonical DNA damage response pathway (Osés-Ruiz et al., 2017; Saunders et al., 2010a). While two cells within the three-celled spore are arrested in interphase, the third, from which the germ tube emerges, undergoes a single round of nuclear division. The ability of the three interconnected cells of the conidium to maintain mitotic autonomy, suggests that septal pore opening and closing may be cell cycle-regulated during appressorium morphogenesis (Shen et al., 2014). Following nuclear division, one of the daughter nuclei is inherited by the, still immature, appressorium, while the other remains in the conidium (Eseola et al., 2021; Osés-Ruiz et al., 2017; Saunders et al., 2010a). To form a penetration-competent appressorium, each of the three cells of the conidium must then undergo regulated cell death, involving both autophagy (Veneault-Fourrey et al., 2006) and ferroptosis (Shen et al., 2020; Shen and Naqvi, 2021), and their contents be recycled and mobilized to meet the metabolic demands of the developing appressorium. While the programmed degradation of the conidium and its contents have been intensively studied (He et al., 2012; Kershaw and Talbot, 2009; Rogers and Egan, 2020; Veneault-Fourrey et al., 2006), less is understood about how a portion of each type of organelle evades destruction and is instead inherited into the developing appressorium, and how this process is spatially and temporally controlled across the three cells of the conidium.

In filamentous fungi, unlike in budding yeast, cytoplasmic microtubules serve as highways for the long-distance bidirectional transport of organelles, mRNA, and other subcellular cargos by, molecular motor proteins (Abenza et al., 2009; Baumann et al., 2014; Egan et al., 2012). Importantly, these microtubule highways are themselves highly dynamic, undergoing periods of stochastic growth and shrinkage from their plus ends (Mitchison and Kirschner, 1984), likely contributing to the capture and transport of diverse organellar cargos (Lomakin et al., 2009). In contrast, the slow-growing minus ends of microtubules are nucleated by large, γ-tubulin-containing complexes, called microtubule-organizing centers. In fungi, the spindle pole body represents the major microtubule organizing center, and is functionally equivalent to the centrosome in higher eukaryotes. In budding yeast, spindle pole bodies are permanently embedded in the nuclear envelope and are the sole sites of nucleation of both cytoplasmic and mitotic microtubules. In fission yeast, however, numerous cell-cycle dependent sites of microtubule nucleation exist (Sawin and Tran, 2006), including equatorial microtubule-organizing centers, which nucleate post-anaphase arrays at the cell-division site during cytokinesis, and interphase microtubule organizing centers which localize along microtubule bundles, on the nuclear envelope and in the cytoplasm (Janson et al., 2005). Importantly, cytoplasmic microtubule nucleation in *Schizosaccharomyces pombe* requires the proteins Mto1 and Mto2 which form a complex promoting the recruitment of the γ-tubulin complex to microtubule organizing sites (Lynch et al., 2013). Cytoplasmic microtubule organizing centers are also present in the yeast-like sporidia of the dimorphic fungus *Ustilago maydis*, where they organize anti-parallel microtubule arrays (Straube et al., 2003). In the model filamentous fungus *Aspergillus nidulans* (Pinheiro et al., 2022), where γ-tubulin itself was first discovered (Oakley and Oakley, 1989), cytoplasmic microtubules are nucleated at both spindle pole bodies and at septa (Gao et al., 2021; Konzack et al., 2005; Xiong and Oakley, 2009; Zhang et al., 2017). Furthermore, *A. nidulans* orthologs of the *S. pombe* proteins, Mto1 and Mto2, termed ApsB and Spa18, respectively, are essential for the recruitment of γ-tubulin ring complex proteins to septal microtubule organizing centers, but not spindle pole bodies (Zhang et al., 2017). Strikingly, septal microtubule organizing centers are also evident in the vegetative hyphae and specialized ring-like adhesive traps of the nematode-trapping fungus, *Duddingtonia flagrans* (Wernet et al., 2021).

Microtubules also form the bipolar mitotic spindle which drives chromosome capture and segregation (Xiang, 2018), a prerequisite for appressorium differentiation by *M. oryzae* (Saunders et al., 2010a). To date, the organization and dynamic behavior of the microtubule cytoskeleton within specialized infective cell types of the blast fungus remain incompletely described (Dulal et al., 2021; Park et al., 2004; Saunders et al., 2010b), yet may have important implications for the understanding of appressorium differentiation, and may inspire new lines of investigation. Here, we use a multicolor fluorescence microscopy-based live-cell imaging approach to describe the organization of cytoplasmic microtubule arrays within infective conidia, provide new insight into the spatial and temporal dynamics of nuclear division and inheritance during appressorium differentiation, and offer a more complete picture of cytoskeletal and nuclear organization in the penetration-primed infection cell.

2. Results and discussion

We generated *M. oryzae* strains co-expressing fluorescent fusion proteins that allowed us to simultaneously image nuclei (Histone H1-tagBFP), microtubules (β-tubulin-GFP), and their dynamic plus-ends (EB1-RFP), within live cells. We isolated conidia, inoculated them into imaging chambers, and generated three-color fluorescence time-lapse sequences to investigate the organization and dynamics of cytoplasmic microtubules within *M. oryzae* cells. Strikingly, we found that cytoplasmic microtubule arrays are organized with their slow growing minus-ends located within the two septa which separate the three cells of the conidium, rather than from spindle pole bodies embedded in the nuclear envelopes (Supplementary Video 1). The emergence of microtubules from septa is similarly apparent in time series acquired during appressorium development, where septin-based structures localized to, what are likely, septal pores (Fig. 1A, dashed box). EB1-labelled microtubule plus-ends grew from both sides of the septa and extended into the cytoplasm (Fig. 1A and C and Supplementary Video 1). Microtubules grew at an average rate of 0.2 μm/s ± 0.1 (SD), consistent with measurements in other eukaryotic cell types (Zwetsloot et al., 2018), and shrank at a faster rate of 0.6 μm/s ± 0.1 (SD) (Fig. 1D). Microtubule shrinkage was most conspicuous after the plus-end reached the cortex (Supplementary Video 1). In the blast fungus, germ tubes most often emerge from the apical cell of the conidium. Based on our data, we speculate that this is likely a consequence of conidium geometry, which promotes the cortex-mediated guidance of polymerizing microtubule plus-ends into the extreme conidium apex (Fig. 1C and Supplementary Video 1), leading to the deposition and accumulation of polarity determinants at this site (Browning et al., 2003) (Fig. 1C and Supplementary Video 1). Consistent with this idea, genetic loss of the cell-end marker Tea4, leads to the emergence of multiple germ tubes from unusual positions on the conidium (Patkar et al., 2010). Kymographs generated from two-color time lapse sequences revealed, as expected, that EB1, a central regulator of microtubule plus-end dynamics (Vaughan, 2005), tracked the tips of growing but not shrinking microtubules in *M. oryzae* cells (Fig. 1D and E) (Bieling et al., 2007). Septum-associated microtubule organizing centers, anchored by intrinsically disordered proteins, have previously been described in the *A. nidulans* (Shukla et al., 2017; Zhang et al., 2017), where they occur alongside canonical spindle pole body-associated microtubule organizing centers within hyphae. Interestingly, the *M. oryzae* genome encodes for likely orthologs of major components of septal microtubule organizing centers in *A. nidulans*, including ApsB (MGG_10857), Spa10 (MGG_07027), and Spa18 (MGG_05218). In *Neurospora crassa*, orthologs of these three proteins also localize to septal pores, however, rather than functioning in the nucleation of microtubule minus ends, they appear to be involved in the anchorage of microtubule plus ends at septal pores (Ramírez-Cota et al., 2022). Thus, the nature and molecular composition of putative septal microtubule organizing centers with *M. oryzae* conidia requires further careful analysis. We hypothesize that microtubule organization within the blast conidium might be optimized for the efficient capture and trafficking of cargos through basal, middle and apical cells during

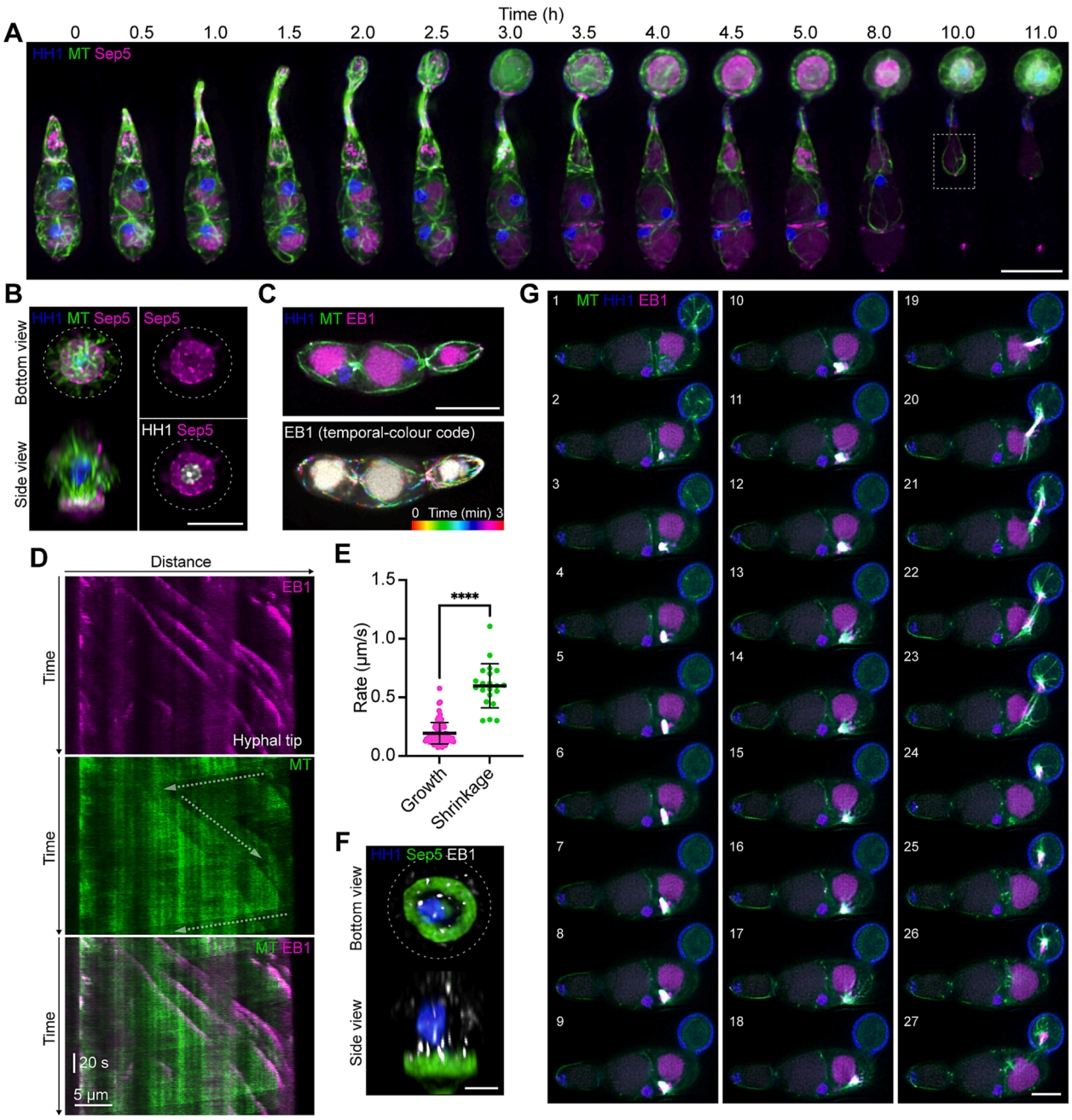

Fig. 1. A. Fluorescence time series highlighting the localization of the microtubule (GFP-β-tubulin) and septin (Sep5-RFP) cytoskeletons, and nuclei (Histone H1-tagBFP), during appressorium development *in vitro*. Dashed box highlights the emergence of cytoplasmic microtubules from a region close to the septal pore, which is labelled by Sep5-RFP. Scale bar = 10 µm. B. Fluorescence micrographs highlighting the organization of the microtubule (β-tubulin-GFP) and septin cytoskeletons (Sep5-RFP), and positioning of the nucleus (Histone H1-tagBFP), in mature penetration-competent appressoria (~16 h.p.i). Scale bar = 10 µm. C. Fluorescence micrograph of a conidia co-expressing EB1-RFP, Histone H1-tagBFP and β-tubulin-GFP (upper panel), and temporally color-coded projections of EB1-RFP comets from Supplementary Video 1. Images were acquired every 1 s, in a single focal plane, for a total of 3 min. Colored lines therefore represent the trajectories of the EB1 comets through time, according to the scale (lower panel). Gamma adjustments were made to panels. Note that RFP persists in the vacuoles resulting in non-specific signal unrelated to EB1 localization. D. Kymographs generated from fluorescence time lapse sequences highlighting the trajectories of EB1-RFP comets (top and bottom panels) which decorate the plus-ends of growing (but not shrinking) cytoplasmic microtubules (middle and bottom panels). Dashed arrows highlight conspicuous growth (towards the hyphal tip) and shrinkage (away from the hyphal tip) events. E. Plot highlighting the rate of microtubule growth (magenta) and shrinkage events (green) in hyphal cells determined from kymographs generated from fluorescence time lapse sequences. Error bars represent standard deviation. $^{****}P < 0.0001$ (Mann Whitney test). F. Fluorescence micrographs highlighting the organization of the septin cytoskeleton (Sep5-RFP), positioning of the nucleus (Histone H1-tagBFP), and localization of microtubule plus-ends (EB1-RFP) in mature penetration-competent appressoria (~16 h.p.i). Scale bar = 2 µm. G. Fluorescence time series, extracted from Supplementary Video 2, highlighting nuclear division during appressorium development *in vitro*. Microtubules are labeled with β-tubulin-GFP, nuclei with Histone H1-tagBFP and microtubule plus-ends with EB1-RFP. Panels are labeled with frame numbers, which were acquired at 30 s intervals. Note non-specific RFP fluorescence in vacuoles and autofluorescence of the incipient appressorium cell wall. Scale bar = 5 µm. Panels A, B and F represent maximum intensity projections of Z-series acquired at 0.2 µm intervals throughout the entire depth of the cell type, while panels C and G represent single Z planes. (For interpretation of the references to color in this figure legend, the reader is referred to the web version of this article.)

appressorium differentiation (Mogre et al., 2021). Importantly, the orientation and organization of microtubules within cellular and multicellular systems dictates the class of motors used to navigate them (Schuster et al., 2011), with cytoplasmic dynein 1 (dynein) moving cargos towards the minus-end, and kinesins moving them towards the plus-end (Egan et al., 2012). In filamentous fungi, and other eukaryotes, dynein accumulates at the microtubule plus-end (Moughamian et al., 2013; Xiang et al., 2000), which serve as a motor-cargo loading zone for some types of organelles (Lenz et al., 2006). It is possible that the microtubules extending into the basal and middle cells of the conidium (Supplementary Video 1), are engaged in the plus-end-mediated "search and capture" of organellar cargos (Lomakin et al., 2009), for their intra- and intercellular transport. However, while various organelles, including peroxisomes and mitochondria, have been shown to migrate into the appressorium during its development (Zhong et al., 2016), it remains unclear whether these are inherited only from the germinating cell, or whether they are transported intercellularly through both septal pores of the conidium. Furthermore, while some classes of organelle have been shown to undergo microtubule-dependent motility during appressorium differentiation, including late endosomes (Ramanujam et al., 2013) and nuclei (Osés-Ruiz et al., 2017; Saunders et al., 2010b), for other classes of organelle, it is not known whether their movement is microtubule-based, or a consequence of bulk cytoplasmic flow (Ramos-García et al., 2009). Interestingly, in both *A. nidulans,* and the corn smut fungus *Ustilago maydis*, some classes of organelle achieve motility by "hitchhiking" on motor-driven early endosomes (Guimaraes et al., 2015; Salogiannis et al., 2016), a process likely requiring cargo specific linkers (Salogiannis et al., 2021; Salogiannis and Reck-Peterson, 2017). Importantly, improved insight into the spatiotemporal dynamics and cellular fate of organelles during appressorium differentiation may inform new strategies to specifically perturb infectious development by the blast fungus. Furthermore, *M. oryzae* may serve as a compelling model system to dissect the mechanism of organelle inheritance in asymmetrically-dividing cells with drastically different fates (Ouellet and Barral, 2012).

Next, we sought to exploit our same fluorescently-tagged strains to gain improved insight into the dynamic reorganization of the microtubule cytoskeleton during nuclear division and inheritance, a prerequisite for appressorium maturation (Saunders et al., 2010a). We imaged germinating conidia, approximately 3 h post inoculation, every 30 s for a period of 3 h in a single focal plane. Prior to the onset of mitosis, cytoplasmic microtubules extended from the basal cell of the conidium, with their EB1-RFP-labelled plus-ends probing the appressorium cortex (Supplementary Video 2, time stamp up to 00.36.00). Soon after, the mitotic spindle emerged as cytoplasmic microtubules within the basal cell of the conidium, and incipient appressorium, rapidly disassembled. The bipolar anaphase spindle migrated towards the incipient appressorium and then re-positioned across the appressorium-germ tube neck (Supplementary Video 2, timestamp 00:47:30), at which point the EB1-RFP-labelled plus-ends of astral microtubules contacted the appressorium cortex (Supplementary Video 2, timestamp 00:48:30). One of the daughter nuclei was then pulled into the appressorium, as cytoplasmic microtubules began to reemerge in the basal cell of the conidium (Supplementary Video 2, timestamp 01.10.00). The nuclei within both the middle and basal cell then disappeared as they likely underwent autophagy (He et al., 2012; Veneault-Fourrey et al., 2006) (Supplementary Video 2, timestamp 01.30.00 onwards). Note that the daughter nucleus within the appressorium migrated out of the focal plane. Panels extracted from Supplementary Video 2 can be seen in Fig. 1G. In budding yeast, positioning of the bipolar anaphase spindle is driven by dynein, which is offloaded to the cell cortex through interaction with its receptor Num1 (Xiang, 2018). Cortically anchored dynein then pulls on astral microtubules, sliding them across the cell cortex, and drawing the connected spindle into the mother bud-neck. Interestingly, the Num1 ortholog in *A. nidulans*, ApsA, was originally identified following a screen for mutants defective in nuclear migration during hyphal growth and conidiation (Clutterbuck, 1994), and thus conserved machinery likely control nuclear positioning in filamentous fungi (Fischer and Timberlake, 1995). Based on our live-cell imaging data (Supplementary Video 2), and previous studies (Pfeifer and Khang, 2020; Saunders et al., 2010a), it seems likely that dynein-dependent forces applied to astral microtubules drive both the migration of one daughter nucleus into the incipient appressorium and the return of the other to the conidium for non-selective autophagic degradation (He et al., 2012; Veneault-Fourrey et al., 2006). Consistent with this idea, deletion of the *M. oryzae* Num1 ortholog perturbs the spatial and temporal control of nuclear division resulting in the formation of non-functional appressoria (Jeon et al., 2014). Interestingly, in budding yeast, Num1 interactions with both mitochondria and the endoplasmic reticulum at the cell cortex are thought to facilitate dynein-mediated spindle positioning (Kraft and Lackner, 2017; Omer et al., 2018). Thus, organelle inheritance is mechanistically coupled to dynein-mediated spindle positioning in some systems. It will be interesting to determine whether organelle localization similarly influences nuclear division, and therefore appressorium differentiation in the blast fungus. Interestingly, following appressorium-mediated cuticle penetration, and during invasive cell-to-cell movement, daughter nuclei must migrate through extremely narrow apertures (Pfeifer and Khang, 2018), leading to unusual spindle geometries (Pfeifer et al., 2019). Continued investigation into the mechanisms of nuclear migration and motility in constrained environments, potentially through the exploitation of microfabricated devices (Bedekovic and Brand, 2022; Hopke et al., 2021), may inform novel control measures.

Lastly, we sought to gain some new perspective on the subcellular organization and architecture of the mature, penetration-poised appressorium through multi-color three-dimensional fluorescence imaging of cytoplasmic microtubules (and their plus-ends), septin-based structures, and post-mitotic nuclei. We inoculated conidia into imaging chambers and incubated them at room temperature for approximately 16 h, by which point they had formed mature appressoria. As expected, the septin cytoskeleton was organized into a higher-order toroidal ring-like structure at the base of the appressorium (Dagdas et al., 2012; Dulal et al., 2021, 2020; Ryder et al., 2013), while a single nucleus was positioned directly above the central pore (Fig. 1B and F). Microtubules were organized in vertical arrays within the appressorium, with their plus-ends orientated towards the septin ring, as previously described (Dulal et al., 2021). While these microtubules did not appear to emerge from the spindle pole body associated with the nucleus (Fig. 1B), careful cell biological analysis of strains expressing additional fluorescent fusion proteins, including those associated with microtubule nucleation (Oakley et al., 1990), will be necessary to better understand cytoskeletal organization in this highly specialized cell type. Critically, high-resolution imaging of appressorium-mediated penetration of yielding surfaces, either synthetic or plant derived, will be essential to understand how these cells are dynamically remodeled to support invasive hyphal growth and further mitotic divisions (Pfeifer and Khang, 2018).

3. Methods

3.1. Fungal maintenance and culture

M. oryzae cultures were maintained on complete media at 25 °C with a 12:12 photoperiod for 10–12 days. Strains were stored as desiccated filter stocks at −20 °C and used to regenerate cultures following three subcultures. All other storage, culture, and media preparation procedures were performed following standard protocol (Molinari and Talbot, 2022).

3.2. Plasmid construction

The histone H1-tagBFP construct was created by modifying an existing histone H1-tdTomato construct (Saunders et al., 2010a),

through replacement of the tdTomato-encoding gene with one encoding for tagBFP (Tan et al., 2014), and transfer of the fusion construct into plasmid pCB1004 (Carroll et al., 1994), containing a hygromycin resistance cassette, by In-Fusion cloning (Takara Bio). The EB1-RFP fusion construct was described previously (Dulal et al., 2021). Cloning strategies, and PCR primers, were designed in Snapgene (version 6.1.1; GSL Biotech).

3.3. Strain construction

Plasmids containing fluorescent fusion protein cassettes were integrated ectopically into the *M. oryzae* genome following polythene glycol-mediated protoplast transformation using established protocols. Transformants containing genomically-integrated constructs were selected based on resistance to sulfonylurea (β-tubulin-GFP), hygromycin (histone H1-BFP), phosphinothricin (Sep5-RFP) or bleomycin (EB1-RFP), conferred by resistance cassettes within backbones pCB1532, pCB1004, pCB1530 (Carroll et al., 1994; Sweigard et al., 1997) and pYP1, respectively. Transformants were passed through two rounds of selection before screening by fluorescence microscopy. Strains were subjected to a single spore isolation before generating filter stocks and storage to ensure homogenous expression of all fluorescently-tagged fusion proteins.

3.4. Live cell imaging and image analysis

Imaging of *M. oryzae* cells was performed as previously described (Rogers et al., 2021).

Fluorescence images of *M. oryzae* cells were acquired on a Nikon Ti-E Eclipse inverted microscope, equipped with a motorized Piezo stage, a Perfect Focus System (Nikon) and, using a 100x 1.49 N.A. oil immersion Apo TIRF Nikon objective. TagBFP, eGFP and RFP were excited using an AURA II triggered illuminator with 405 nm, 485 nm and 560 nm light-emitting diodes, respectively, and fluorescence detected using a Zyla 4.2 sCMOS camera (Andor Technology). All hardware was controlled by NIS-Elements Advanced Research (version 4.60). Live-cell imaging was performed at room temperature (21–23 °C). Three-color time lapse data sets were deconvolved, with spherical aberration correction and background subtraction, using the "Automatic" 3D (or 2D) deconvolution option in NIS-Elements Advanced Research. Maximum intensity projection of three-color Z-series shown in Fig. 1A and B were generated in Imaris 9.5.1 (Bitplane), and exported as TIFs using the "Snapshot" function. All data were plotted in Prism 8 (version 8.2.1; Graphpad). Kymographs were generated in Fiji/ImageJ2 (version:2.3.0/1.53f) (Rueden et al., 2017) by drawing a segmented line over the trajectory of an EB1 comet in a maximum intensity projection of a two-color fluorescence time lapse sequence, and using the Image > Stacks > Reslice function. Microtubule growth and shrinkage rates measured using the kymograph plugin. Videos were created and annotated in Fiji/ImageJ2 (version:2.3.0/1.53f).

Acknowledgements

We thank Jin-rong Xu (Purdue University, USA) for sharing plasmid pYP1, and Nick Talbot (The Sainsbury Laboratory, UK) for sharing a histone-h1-tdTomato plasmid (Saunders et al., 2010b). M.J.E is supported by NSF CAREER Award Number: 2141858.

Appendix A. Supplementary material

Supplementary data to this article can be found online at https://doi.org/10.1016/j.fgb.2022.103768.

References

Abenza, J.F., Pantazopoulou, A., Rodríguez, J.M., Galindo, A., Peñalva, M.A., 2009. Long-Distance Movement of Aspergillus nidulans Early Endosomes on Microtubule Tracks. Traffic 10, 57–75. https://doi.org/10.1111/j.1600-0854.2008.00848.x.

Anjago, W.M., Zhou, T., Zhang, H., Shi, M., Yang, T., Zheng, H., Wang, Z., 2018. Regulatory network of genes associated with stimuli sensing, signal transduction and physiological transformation of appressorium in Magnaporthe oryzae. Mycol 9, 1–12. https://doi.org/10.1080/21501203.2018.1492981.

Baumann, S., König, J., Koepke, J., Feldbrügge, M., 2014. Endosomal transport of septin mRNA and protein indicates local translation on endosomes and is required for correct septin filamentation. Embo Rep. 15, 94–102. https://doi.org/10.1002/embr.201338037.

Bedekovic, T., Brand, A.C., 2022. Microfabrication and its use in investigating fungal biology. Mol. Microbiol. 117, 569–577. https://doi.org/10.1111/mmi.14816.

Bieling, P., Laan, L., Schek, H., Munteanu, E.L., Sandblad, L., Dogterom, M., Brunner, D., Surrey, T., 2007. Reconstitution of a microtubule plus-end tracking system in vitro. Nature 450, 1100–1105. https://doi.org/10.1038/nature06386.

Browning, H., Hackney, D.D., Nurse, P., 2003. Targeted movement of cell end factors in fission yeast. Nat. Cell Biol. 5, 812–818. https://doi.org/10.1038/ncb1034.

Carroll, A.M., Sweigard, J.A., Valent, B., 1994. Improved Vectors for Selecting Resistance to Hygromycin. Fungal Genet. Rep. 41, 22. https://doi.org/10.4148/1941-4765.1367.

Clutterbuck, A.J., 1994. Mutants of Aspergillus nidulans deficient in nuclear migration during hyphal growth and conidiation. Microbiology+ 140, 1169–1174. https://doi.org/10.1099/13500872-140-5-1169.

Dagdas, Y.F., Yoshino, K., Dagdas, G., Ryder, L.S., Bielska, E., Steinberg, G., Talbot, N.J., 2012. Septin-Mediated Plant Cell Invasion by the Rice Blast Fungus, Magnaporthe oryzae. Science 336, 1590–1595. https://doi.org/10.1126/science.1222934.

de Jong, J.C., McCormack, B.J., Smirnoff, N., Talbot, N.J., 1997. Glycerol generates turgor in rice blast. Nature 389, 244. https://doi.org/10.1038/38418.

Dulal, N., Rogers, A., Wang, Y., Egan, M., 2020. Dynamic assembly of a higher-order septin structure during appressorium morphogenesis by the rice blast fungus. Fungal Genet. Biol. 140, 103385 https://doi.org/10.1016/j.fgb.2020.103385.

Dulal, N., Rogers, A.M., Proko, R., Bieger, B.D., Liyanage, R., Krishnamurthi, V.R., Wang, Y., Egan, M.J., 2021. Turgor-dependent and coronin-mediated F-actin dynamics drive septin disc-to-ring remodeling in the blast fungus Magnaporthe oryzae. J. Cell Sci. 134, jcs251298. https://doi.org/10.1242/jcs.251298.

Egan, M.J., Wang, Z.-Y., Jones, M.A., Smirnoff, N., Talbot, N.J., 2007. Generation of reactive oxygen species by fungal NADPH oxidases is required for rice blast disease. Proc. Natl. Acad. Sci. 104, 11772–11777. https://doi.org/10.1073/pnas.0700574104.

Egan, M.J., McClintock, M.A., Reck-Peterson, S.L., 2012. Microtubule-based transport in filamentous fungi. Curr. Opin. Microbiol. 15, 637–645. https://doi.org/10.1016/j.mib.2012.10.003.

Eseola, A.B., Ryder, L.S., Osés-Ruiz, M., Findlay, K., Yan, X., Cruz-Mireles, N., Molinari, C., Garduño-Rosales, M., Talbot, N.J., 2021. Investigating the cell and developmental biology of plant infection by the rice blast fungus Magnaporthe oryzae. Fungal Genet. Biol. 154, 103562 https://doi.org/10.1016/j.fgb.2021.103562.

Fischer, R., Timberlake, W.E., 1995. Aspergillus nidulans apsA (anucleate primary sterigmata) encodes a coiled-coil protein required for nuclear positioning and completion of asexual development. J. Cell Biol. 128, 485–498. https://doi.org/10.1083/jcb.128.4.485.

Gao, X., Herrero, S., Wernet, V., Erhardt, S., Valerius, O., Braus, G.H., Fischer, R., 2021. The role of Aspergillus nidulans polo-like kinase PlkA in microtubule-organizing center control. J. Cell Sci. 134 https://doi.org/10.1242/jcs.256537.

Guimaraes, S.C., Schuster, M., Bielska, E., Dagdas, G., Kilaru, S., Meadows, B.R.A., Schrader, M., Steinberg, G., 2015. Peroxisomes, lipid droplets, and endoplasmic reticulum "hitchhike" on motile early endosomes. J. Cell Biol. 211, 945–954. https://doi.org/10.1083/jcb.201505086.

He, M., Kershaw, M.J., Soanes, D.M., Xia, Y., Talbot, N.J., 2012. Infection-Associated Nuclear Degeneration in the Rice Blast Fungus Magnaporthe oryzae Requires Non-Selective Macro-Autophagy. PLoS One 7 (3), e33270.

Hopke, A., Mela, A., Ellett, F., Carter-House, D., Peña, J.F., Stajich, J.E., Altamirano, S., Lovett, B., Egan, M., Kale, S., Kronholm, I., Guerette, P., Szewczyk, E., McCluskey, K., Breslauer, D., Shah, H., Coad, B.R., Momany, M., Irimia, D., 2021. Crowdsourced analysis of fungal growth and branching on microfluidic platforms. PLoS One 16 (9), e0257823.

Janson, M.E., Setty, T.G., Paoletti, A., Tran, P.T., 2005. Efficient formation of bipolar microtubule bundles requires microtubule-bound γ-tubulin complexes. J. Cell Biol. 169, 297–308. https://doi.org/10.1083/jcb.200410119.

Jeon, J., Rho, H., Kim, S., Kim, K.S., Lee, Y.-H., 2014. Role of MoAND1-mediated nuclear positioning in morphogenesis and pathogenicity in the rice blast fungus, Magnaporthe oryzae. Fungal Genet. Biol. 69, 43–51. https://doi.org/10.1016/j.fgb.2014.05.002.

Kershaw, M.J., Talbot, N.J., 2009. Genome-wide functional analysis reveals that infection-associated fungal autophagy is necessary for rice blast disease. Proc. Natl. Acad. Sci. 106, 15967–15972. https://doi.org/10.1073/pnas.0901477106.

Konzack, S., Rischitor, P.E., Enke, C., Fischer, R., 2005. The Role of the Kinesin Motor KipA in Microtubule Organization and Polarized Growth of Aspergillus nidulans. Mol. Biol. Cell 16, 497–506. https://doi.org/10.1091/mbc.e04-02-0083.

Kraft, L.M., Lackner, L.L., 2017. Mitochondria-driven assembly of a cortical anchor for mitochondria and dynein. J. Cell Biol. 216, 3061–3071. https://doi.org/10.1083/jcb.201702022.

Lenz, J.H., Schuchardt, I., Straube, A., Steinberg, G., 2006. A dynein loading zone for retrograde endosome motility at microtubule plus-ends. Embo J. 25, 2275–2286. https://doi.org/10.1038/sj.emboj.7601119.

Lomakin, A.J., Semenova, I., Zaliapin, I., Kraikivski, P., Nadezhdina, E., Slepchenko, B. M., Akhmanova, A., Rodionov, V., 2009. CLIP-170-Dependent Capture of Membrane Organelles by Microtubules Initiates Minus-End Directed Transport. Dev. Cell 17, 323–333. https://doi.org/10.1016/j.devcel.2009.07.010.

Lynch, E.M., Groocock, L.M., Borek, W.E., Sawin, K.E., 2013. Activation of the γ-tubulin complex by the Mto1/2 complex. Curr. Biol. Cb 24, 896–903. https://doi.org/10.1016/j.cub.2014.03.006.

Mitchison, T., Kirschner, M., 1984. Dynamic instability of microtubule growth. Nature 312, 237–242. https://doi.org/10.1038/312237a0.

Mogre, S.S., Christensen, J.R., Reck-Peterson, S.L., Koslover, E.F., 2021. Optimizing microtubule arrangements for rapid cargo capture. Biophys. J. 120, 4918–4931. https://doi.org/10.1016/j.bpj.2021.10.020.

Molinari, C., Talbot, N.J., 2022. A Basic Guide to the Growth and Manipulation of the Blast Fungus. Magnaporthe oryzae. Curr Protoc 2, e523.

Money, N.P., Howard, R.J., 1996. Confirmation of a Link between Fungal Pigmentation, Turgor Pressure, and Pathogenicity Using a New Method of Turgor Measurement. Fungal Genet. Biol. 20, 217–227. https://doi.org/10.1006/fgbi.1996.0037.

Moughamian, A.J., Osborn, G.E., Lazarus, J.E., Maday, S., Holzbaur, E.L.F., 2013. Ordered Recruitment of Dynactin to the Microtubule Plus-End is Required for Efficient Initiation of Retrograde Axonal Transport. J. Neurosci. 33, 13190–13203. https://doi.org/10.1523/jneurosci.0935-13.2013.

Oakley, C.E., Oakley, B.R., 1989. Identification of γ-tubulin, a new member of the tubulin superfamily encoded by mipA gene of Aspergillus nidulans. Nature 338, 662–664. https://doi.org/10.1038/338662a0.

Oakley, B.R., Oakley, C.E., Yoon, Y., Jung, M.K., 1990. γ-tubulin is a component of the spindle pole body that is essential for microtubule function in Aspergillus nidulans. Cell 61, 1289–1301. https://doi.org/10.1016/0092-8674(90)90693-9.

Omer, S., Greenberg, S.R., Lee, W.-L., 2018. Cortical dynein pulling mechanism is regulated by differentially targeted attachment molecule Num1. Elife 7, e36745.

Osés-Ruiz, M., Sakulkoo, W., Littlejohn, G.R., Martin-Urdiroz, M., Talbot, N.J., 2017. Two independent S-phase checkpoints regulate appressorium-mediated plant infection by the rice blast fungus Magnaporthe oryzae. Proc. Natl. Acad. Sci. 114, E237–E244. https://doi.org/10.1073/pnas.1611307114.

Ouellet, J., Barral, Y., 2012. Organelle segregation during mitosis: Lessons from asymmetrically dividing cells. J. Cell Biol. 196, 305–313. https://doi.org/10.1083/jcb.201102078.

Park, G., Bruno, K.S., Staiger, C.J., Talbot, N.J., Xu, J., 2004. Independent genetic mechanisms mediate turgor generation and penetration peg formation during plant infection in the rice blast fungus. Mol. Microbiol. 53, 1695–1707. https://doi.org/10.1111/j.1365-2958.2004.04220.x.

Patkar, R.N., Suresh, A., Naqvi, N.I., 2010. MoTea4-Mediated Polarized Growth Is Essential for Proper Asexual Development and Pathogenesis in Magnaporthe oryzae. Eukaryot. Cell 9, 1029–1038. https://doi.org/10.1128/ec.00292-09.

Pfeifer, M.A., Jones, K., Khang, C.H., 2019. A strikingly-angled spindle mediates nuclear migration during colonization of rice cells infected by Magnaporthe oryzae. Fungal Genet. Biol. 126, 56–60. https://doi.org/10.1016/j.fgb.2019.02.005.

Pfeifer, M.A., Khang, C.H., 2018. A nuclear contortionist: the mitotic migration of Magnaporthe oryzae nuclei during plant infection. Mycol 9, 202–210. https://doi.org/10.1080/21501203.2018.1482966.

Pfeifer, M.A., Khang, C.H., 2020. Nup84 persists within the nuclear envelope of the rice blast fungus, Magnaporthe oryzae, during mitosis. Fungal Genet. Biol. 146, 103472 https://doi.org/10.1016/j.fgb.2020.103472.

Pinheiro, Â., Piontkivska, D., Sequeira, P., Martins, T.M., Pereira, C.S., 2022. Aspergillus nidulans. Trends Microbiol. https://doi.org/10.1016/j.tim.2022.09.013.

Ramanujam, R., Calvert, M.E., Selvaraj, P., Naqvi, N.I., 2013. The Late Endosomal HOPS Complex Anchors Active G-Protein Signaling Essential for Pathogenesis in Magnaporthe oryzae. Plos Pathog. 9 (8), e1003527.

Ramírez-Cota, R., Espino-Vazquez, A.N., Rodriguez-Vega, T.C., Macias-Díaz, R.E., Callejas-Negrete, O.A., Freitag, M., Fischer, R., Roberson, R.W., Mouriño-Pérez, R.R., 2022. The cytoplasmic microtubule array in Neurospora crassa depends on microtubule-organizing centers at spindle pole bodies and microtubule +end-depending pseudo-MTOCs at septa. Fungal Genet Biol 162, 103729. https://doi.org/10.1016/j.fgb.2022.103729.

Ramos-García, S.L., Roberson, R.W., Freitag, M., Bartnicki-García, S., Mouriño-Pérez, R. R., 2009. Cytoplasmic bulk flow propels nuclei in mature hyphae of Neurospora crassa. Eukaryot Cell 8, 1880–1890. https://doi.org/10.1128/ec.00062-09.

Rogers, A., Dulal, N., Egan, M., 2021. Magnaporthe oryzae, Methods and Protocols. Methods Mol Biology 2356, 87–96. https://doi.org/10.1007/978-1-0716-1613-0_7.

Rogers, A.M., Egan, M.J., 2020. Autophagy machinery promotes the chaperone-mediated formation and compartmentalization of protein aggregates during appressorium development by the rice blast fungus. Mol Biol Cell 31 (21), 2298–2305.

Rueden, C.T., Schindelin, J., Hiner, M.C., DeZonia, B.E., Walter, A.E., Arena, E.T., Eliceiri, K.W., 2017. Image J2: ImageJ for the next generation of scientific image data. BMC Bioinf. 18, 529. https://doi.org/10.1186/s12859-017-1934-z.

Ryder, L.S., Dagdas, Y.F., Mentlak, T.A., Kershaw, M.J., Thornton, C.R., Schuster, M., Chen, J., Wang, Z., Talbot, N.J., 2013. NADPH oxidases regulate septin-mediated cytoskeletal remodeling during plant infection by the rice blast fungus. Proc National Acad Sci 110, 3179–3184. https://doi.org/10.1073/pnas.1217470110.

Ryder, L.S., Dagdas, Y.F., Kershaw, M.J., Venkataraman, C., Madzvamuse, A., Yan, X., Cruz-Mireles, N., Soanes, D.M., Oses-Ruiz, M., Styles, V., Sklenar, J., Menke, F.L.H., Talbot, N.J., 2019. A sensor kinase controls turgor-driven plant infection by the rice blast fungus. Nature 574, 423–427. https://doi.org/10.1038/s41586-019-1637-x.

Ryder, L.S., Cruz-Mireles, N., Molinari, C., Eisermann, I., Eseola, A.B., Talbot, N.J., 2022. The appressorium at a glance. J Cell Sci 135. https://doi.org/10.1242/jcs.259857.

Salogiannis, J., Egan, M.J., Reck-Peterson, S.L., 2016. Peroxisomes move by hitchhiking on early endosomes using the novel linker protein PxdA. J Cell Biol 212, 289–296. https://doi.org/10.1083/jcb.201512020.

Salogiannis, J., Christensen, J.R., Songster, L.D., Aguilar-Maldonado, A., Shukla, N., Reck-Peterson, S.L., 2021. PxdA interacts with the DipA phosphatase to regulate peroxisome hitchhiking on early endosomes. Mol Biol Cell 32 (6), 492–503.

Salogiannis, J., Reck-Peterson, S.L., 2017. Hitchhiking: A Non-Canonical Mode of Microtubule-Based Transport. Trends Cell Biol 27, 141–150. https://doi.org/10.1016/j.tcb.2016.09.005.

Saunders, D.G.O., Aves, S.J., Talbot, N.J., 2010a. Cell Cycle-Mediated Regulation of Plant Infection by the Rice Blast Fungus. Plant Cell 22, 497–507. https://doi.org/10.1105/tpc.109.072447.

Saunders, D.G.O., Dagdas, Y.F., Talbot, N.J., 2010b. Spatial Uncoupling of Mitosis and Cytokinesis during Appressorium-Mediated Plant Infection by the Rice Blast Fungus Magnaporthe oryzae. Plant Cell 22, 2417–2428. https://doi.org/10.1105/tpc.110.074492.

Sawin, K.E., Tran, P.T., 2006. Cytoplasmic microtubule organization in fission yeast. Yeast 23, 1001–1014. https://doi.org/10.1002/yea.1404.

Schuster, M., Kilaru, S., Fink, G., Collemare, J., Roger, Y., Steinberg, G., 2011. Kinesin-3 and dynein cooperate in long-range retrograde endosome motility along a nonuniform microtubule array. Mol Biol Cell 22 (19), 3645–3657.

Shen, Q., Liang, M., Yang, F., Deng, Y.Z., Naqvi, N.I., 2020. Ferroptosis contributes to developmental cell death in rice blast. New Phytol 227, 1831–1846. https://doi.org/10.1111/nph.16636.

Shen, Q., Naqvi, N.I., 2021. Ferroptosis and microbial pathogenesis. Plos Pathog 17 (3), e1009298.

Shen, K.-F., Osmani, A.H., Govindaraghavan, M., Osmani, S.A., 2014. Mitotic regulation of fungal cell-to-cell connectivity through septal pores involves the NIMA kinase. Mol Biol Cell 25 (6), 763–775.

Shukla, N., Osmani, A.H., Osmani, S.A., 2017. Microtubules are reversibly depolymerized in response to changing gaseous microenvironments within Aspergillus nidulans biofilms. Mol Biol Cell 28 (5), 634–644.

Straube, A., Brill, M., Oakley, B.R., Horio, T., Steinberg, G., 2003. Microtubule Organization Requires Cell Cycle-dependent Nucleation at Dispersed Cytoplasmic Sites: Polar and Perinuclear Microtubule Organizing Centers in the Plant Pathogen Ustilago maydis. Mol Biol Cell 14 (2), 642–657.

Sweigard, J.A., Chumley, F., Carroll, A., Farrall, L., Valent, B., 1997. A series of vectors for fungal transformation. Fungal Genet. Rep. 44, 52–53. https://doi.org/10.4148/1941-4765.1287.

Tan, K., Roberts, A.J., Chonofsky, M., Egan, M.J., Reck-Peterson, S.L., 2014. A microscopy-based screen employing multiplex genome sequencing identifies cargo-specific requirements for dynein velocity. Mol. Biol Cell. 25 (5), 669–678.

Vaughan, K.T., 2005. TIP maker and TIP marker; EB1 as a master controller of microtubule plus ends. J. Cell Biol. 171, 197–200. https://doi.org/10.1083/jcb.200509150.

Veneault-Fourrey, C., Barooah, M., Egan, M., Wakley, G., Talbot, N.J., 2006. Autophagic Fungal Cell Death Is Necessary for Infection by the Rice Blast Fungus. Science 312, 580–583. https://doi.org/10.1126/science.1124550.

Wernet, V., Wäckerle, J., Fischer, R., 2021. The STRIPAK component SipC is involved in morphology and cell-fate determination in the nematode-trapping fungus Duddingtonia flagrans. Genetics 220, iyab153-. https://doi.org/10.1093/genetics/iyab153.

Xiang, X., 2018. Nuclear movement in fungi. Semin. Cell Dev. Biol. 82, 3–16. https://doi.org/10.1016/j.semcdb.2017.10.024.

Xiang, X., Han, G., Winkelmann, D.A., Zuo, W., Morris, N.R., 2000. Dynamics of cytoplasmic dynein in living cells and the effect of a mutation in the dynactin complex actin-related protein Arp1. Curr. Biol. 10, 603–606. https://doi.org/10.1016/s0960-9822(00)00488-7.

Xiong, Y., Oakley, B.R., 2009. In vivo analysis of the functions of γ-tubulin-complex proteins. J. Cell Sci. 122, 4218–4227. https://doi.org/10.1242/jcs.059196.

Zhang, Y., Gao, X., Manck, R., Schmid, M., Osmani, A.H., Osmani, S.A., Takeshita, N., Fischer, R., 2017. Microtubule-organizing centers of Aspergillus nidulans are anchored at septa by a disordered protein. Mol. Microbiol. 106, 285–303. https://doi.org/10.1111/mmi.13763.

Zhong, K., Li, X., Le, X., Kong, X., Zhang, H., Zheng, X., Wang, P., Zhang, Z., Thomma, B., 2016. MoDnm1 Dynamin Mediating Peroxisomal and Mitochondrial Fission in Complex with MoFis1 and MoMdv1 Is Important for Development of Functional Appressorium in Magnaporthe oryzae. Plos Pathog. 12 (8), e1005823.

Zwetsloot, A.J., Tut, G., Straube, A., 2018. Measuring microtubule dynamics. Essays Biochem. 62, 725–735. https://doi.org/10.1042/ebc20180035.